

Thermally activated recovery of electrical conductivity in $\text{LaAlO}_3/\text{SrTiO}_3$

Snir Seri, Moty Schultz, and Lior Klein

*Department of Physics, Nano-magnetism Research Center,
Institute of Nanotechnology and Advanced Materials, Bar-Ilan University, Ramat-Gan 52900, Israel*

Patterned structures of $\text{LaAlO}_3/\text{SrTiO}_3$ that exhibit a decrease in their electrical conductivity below 30 K, recover their higher conductivity upon warming in a thermally activated process. Two dominant energy barriers E_b are identified: $E_{b1} = 0.224 \pm 0.003$ eV related to conductivity recovery near 70 K and $E_{b2} = 0.44 \pm 0.015$ eV related to conductivity recovery near 160 K. We discuss possible linkage to structural defects such as dislocations and twin boundaries.

PACS numbers:

An attractive feature of the interface between the insulating oxides SrTiO_3 and LaAlO_3 (LAO/STO) [1, 2] is the ability to tune its transport properties by gate voltage [3–10]. However, it appears that there are other mechanisms that yield effectively the same effect without gating, including similar correlations between sheet resistance, carrier density and mobility. In a recent report [11], we showed that LAO/STO patterns with current path width smaller than 10 microns may exhibit below 30 K a significant decrease in their electrical conductivity, in connection with driving a sufficiently large current through the sample and/or applying an in-plane magnetic field. The initial high conductivity is recoverable upon applying a warming cycle.

Concomitantly with the field- and current-induced decrease in conductivity, the sheet carrier density (n_s) and mobility decrease, magnetotransport features linked to magnetism [12–14] are suppressed, and the nonuniformity of the sample increases. Namely, without applying a gate voltage, there are mechanisms that decrease conductivity. Furthermore, the mechanism also increases the nonuniformity of the conductivity, a feature that was directly observed with scanning probe microscopy [15, 16].

Here, we explore in detail the time and temperature dependence of the conductivity recovery as the sample is warmed up and show that it is well described by a thermally activated process. We extract two energy barriers: $E_{b1} = 0.224 \pm 0.003$ eV for the conductivity recovery near 70 K and $E_{b2} = 0.44 \pm 0.015$ eV for the conductivity recovery near 160 K. The conductivity exhibits a noticeable time dependence also above room temperature; however, it can not be correlated with a single thermally-activated process.

The results not only provide an explanation for a puzzling behavior reported previously [17, 18], they also provide quantitative details on what appears to be a low-temperature charge trapping mechanism that reduces the carrier density and increases nonuniformity. Thus, they provide new insights regarding two of the main issues concerning the transport properties of the LAO/STO interface: the existence and nature of localized charge carriers [19–21], and the origins of interface nonuniformity [12, 15, 16]. The identified energy scales and length scales

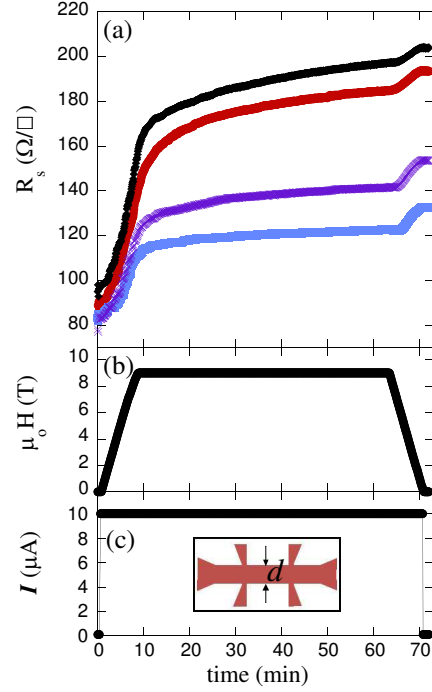


FIG. 1: (a) The sheet resistance (R_s) vs time at 5 K in a pattern with $d = 10 \mu\text{m}$. (b) The time dependence of a magnetic field applied parallel to the LAO/STO interface. (c) The time dependence of a current driven through the pattern. Inset: A sketch of a typical pattern.

are instrumental in identifying the trapping sites which would enable better understanding and control of the transport properties of the LAO/STO interface. Based on the relevant length scale of the phenomenon, we suggest that the trapping sites might be linked to crystal imperfections with similar length scales, such as dislocations and twin boundaries. Interestingly, a recent report shows accelerated recovery of conductivity (after its suppression with gating) in $\text{LaTiO}_3/\text{SrTiO}_3$ system at temperatures close to 70 and 160 K [22], raising the possibility that the relevance of the reported phenomenon exceeds the LAO/STO interface.

The samples were grown by pulsed laser deposition in an oxygen atmosphere of 7×10^{-5} mbar on TiO_2 termi-

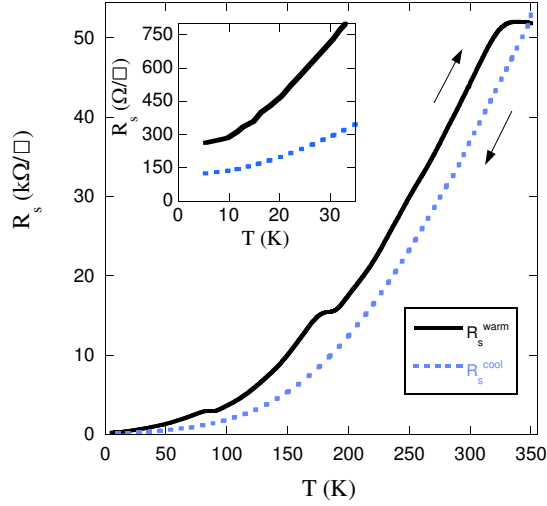


FIG. 2: The sheet resistance (R_s) as a function of temperature during cooling (dashed line, blue) and during warming (solid line, black) after increasing R_s at 5 K (using the procedures shown in Fig. 1). Inset: Blow up of the low temperature data.

nated (001) STO surfaces at 770° C. The LAO thickness is 4 unit cells. The samples were cooled to room temperature in 400 mbars of O₂, including one hour oxidation step at 600° C. The laser fluence was about 0.8 J/cm², with repetition rate of 1 Hz. Patterning was done by photolithography as described in Ref. [23]. Typical geometry of our samples is shown in Fig. 1c (inset). The current path width (d) in the patterns used for this research is 5 and 10 μ m. The contact arrangement allows for simultaneous longitudinal and transverse voltage measurements.

Figure 1 shows typical protocols used to increase the sheet resistance R_s at 5 K of a pattern with a current path width $d = 10 \mu$ m. The figure shows the time dependence of R_s while a current of 10 μ A is driven through the pattern and a magnetic field is applied parallel to the LAO/STO interface (see Figs. 1b and 1c). Before and after the application of the high current and the high in-plane field, R_s is measured with a low current (0.1 μ A) and a zero magnetic field. The different curves in Fig. 1a are obtained with the same pattern in different cooling cycles. We note that the induced increase in R_s may vary significantly in different cooling cycles.

Figure 2 shows the temperature dependence of R_s during cooling (dashed line, blue) and warming (solid line, black) after applying at 5 K the protocols to increase R_s as shown in Figure 1. The temperature is changed continuously at a rate of about 8 K/min both in cooling and warming. The breaks in the warming curve near 70 and 160 K suggest an accelerated decrease of R_s . To understand its nature, we focus on the time dependence of R_s in the vicinity of the two temperatures.

Figures 3a and 3b show R_s as a function of time (after a low-temperature increase in R_s) as the temperature is

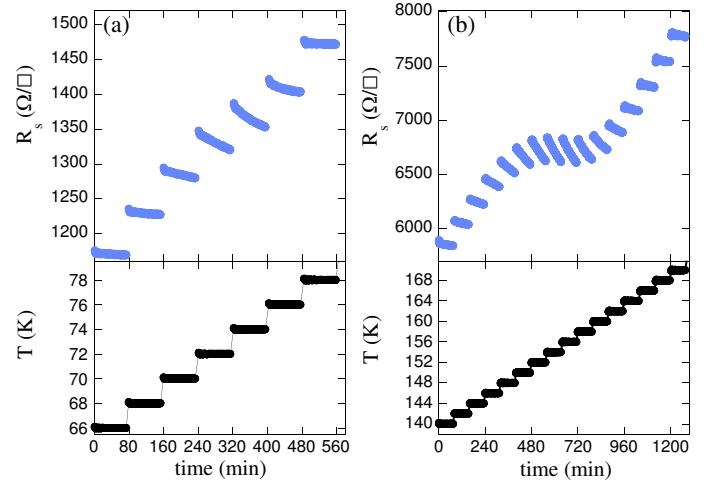


FIG. 3: The sheet resistance (R_s) as a function of time after increasing R_s at 5 K (see Fig. 1), as the temperature is increased in steps near 70 K (a) and 160 K (b).

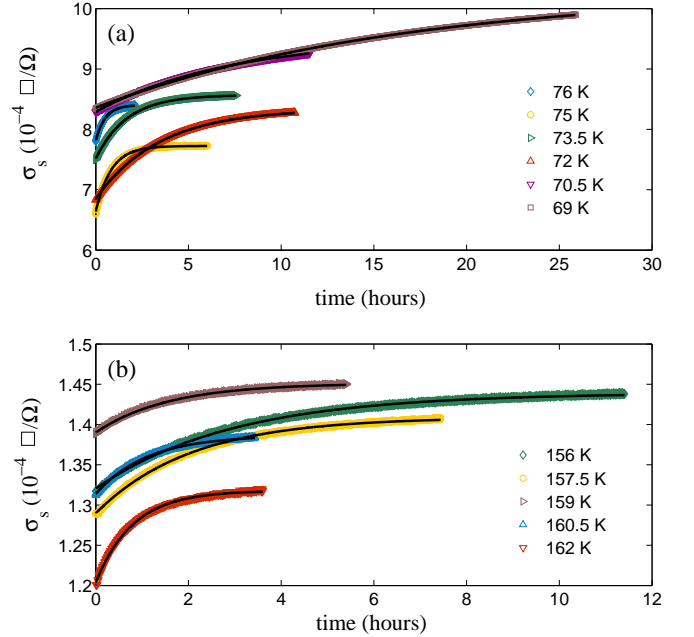


FIG. 4: The sheet conductivity (σ_s) as a function of time after increasing R_s at 5 K (see Fig. 1), at different temperatures near 70 K (a) and 160 K (b). After each measurement, R_s was recovered to its as-cooled value by warming the sample to 350 K. The lines are fits to Eq. 4.

increased in steps near 70 and 160 K, respectively. For the two temperature intervals, the recovery rate increases with increasing temperature until it saturates.

Figures 4a and 4b demonstrate the recovery in a different way. They show the time dependence of the sheet conductivity σ_s at different temperatures near 70 and 160

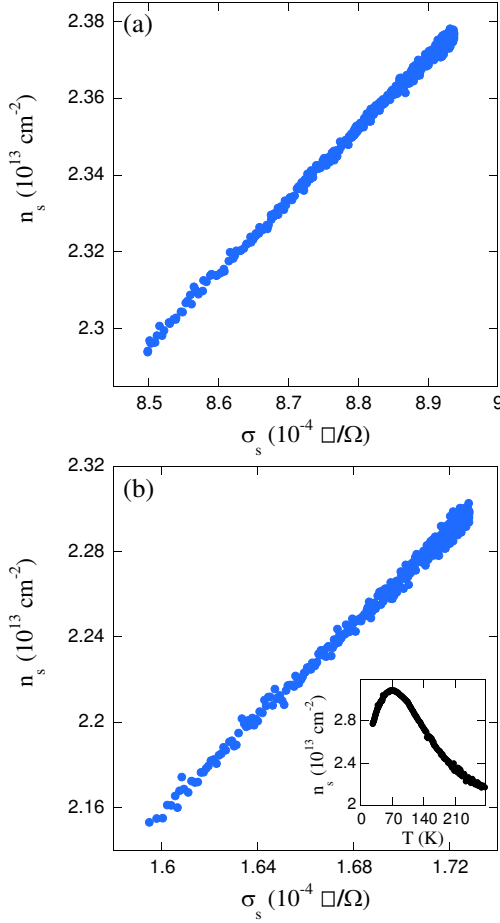


FIG. 5: The sheet carrier density (n_s) as a function of the sheet conductivity (σ_s) at 75 K (a) and 160.5 K (b). Inset: The temperature dependence of n_s in the relevant temperature range during cooling.

K where each measurement is performed after warming the sample to 350 K, cooling it to 5 K, and increasing its sheet resistance as shown in Fig. 1. The same protocol was used for all measurements. Nevertheless, non-monotonic behavior of σ_s as a function of temperature is observed in Figs. 4a and 4b due to the different induced R_s increases obtained in the different cooling cycles, as shown in Fig. 1.

Figures 5a and 5b show the change in the sheet carrier density n_s , extracted from Hall effect measurements, as a function of σ_s as it recovers with time at 75 and 160.5 K, respectively. The inset of Figure 5b shows the temperature dependence of the extracted n_s in the relevant temperature range during cooling the sample, when no relaxation effects exist. The Hall effect resistance was extracted by exchanging the current and voltage leads without reversing the field, as described in Ref. [12]. For the Hall measurements we apply perpendicular fields up to 9 T with no observable effect on the rate of the conductivity recovery. We note that there is a linear correlation between n_s and σ_s during the conductivity recovery;

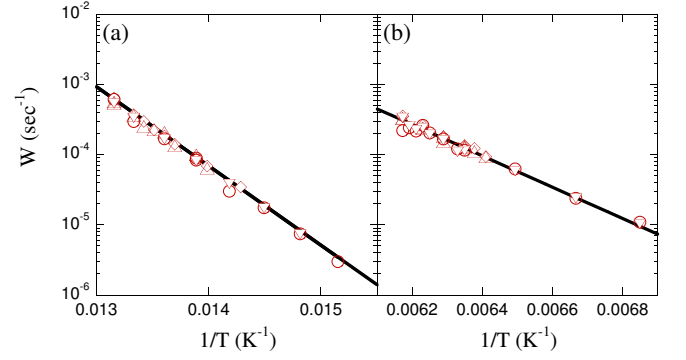


FIG. 6: The parameter W (Eq. 4) as a function of $1/T$ near 70 K (a) and 160 K (b). Different symbols represent different patterns. The lines are fits to Eq. 5.

therefore, to describe the conductivity recovery we may use a model for the time dependence of n_s .

We assume that the low-temperature increase in R_s is due to induced trapping of charge carriers and that the high-temperature recovery is due to their thermally-activated release. The corresponding rate equations are

$$\frac{dN_1}{dt} = -W_{12} \cdot N_1 + W_{21} \cdot N_2 \quad (1)$$

$$\frac{dN_2}{dt} = W_{12} \cdot N_1 - W_{21} \cdot N_2 \quad (2)$$

where N_1 and N_2 are the number of trapped and untrapped charge carriers, respectively, and W_{12} (W_{21}) is the probability for a trapped (untrapped) charge carrier to be released (trapped).

Considering the linear dependence between σ and n_s during the conductivity recovery, we obtain

$$\frac{d\sigma}{dt} \propto (N_1^0 \cdot W_{12} - N_2^0 \cdot W_{21}) \cdot e^{-W \cdot t} \quad (3)$$

where N_1^0 (N_2^0) is the initial number of the trapped (untrapped) charge carriers and $W = W_{12} + W_{21}$.

From here we find that

$$\sigma(t) = -A \cdot e^{-W \cdot t} + B \quad (4)$$

where the coefficient B is the conductivity at $t \rightarrow \infty$ and $A = \sigma_{t \rightarrow \infty} - \sigma_{t=0}$. The lines in Figures 4a and 4b are fits to Eq. 4.

Figures 6a and 6b show the parameter W [Eq. 4] in a logarithmic scale as a function of $1/T$ near 70 and 160 K, respectively, extracted by analyzing the time-dependent conductivity of several patterns of two different samples. The clear linear dependence indicates

$$W = f_0 \cdot e^{-E_b/k_B T} \quad (5)$$

suggesting an Arrhenius-type behavior. The lines in Figs. 6a and 6b are fits to Eq. 5.

We identify two dominant energy barriers: $E_{b1} = 0.224 \pm 0.003$ eV related to conductivity recovery near 70 K and $E_{b2} = 0.44 \pm 0.015$ eV related to conductivity recovery near 160 K. The value of f_0 is on the order of 10^{11} s^{-1} for the conductivity recovery near 70 K and on the order of 10^{10} s^{-1} for the conductivity recovery near 160 K.

The time dependence of the conductivity above room temperature is more complicated and pattern dependent. In several patterns, the conductivity increases initially; however, after some time it starts decreasing and appears to saturate. This may indicate that the time dependence of the conductivity above room temperature is affected by several processes. We note that assuming two competing relaxation processes yields

$$\sigma(t) = -A \cdot e^{-W \cdot t} + A' \cdot e^{-W' \cdot t} + B. \quad (6)$$

which fits the data quite well. However, the fitting parameters are strongly pattern dependent so no clear conclusion can be obtained.

Based on our measurements, a plausible scenario is that the current- and field-induced suppression of conductivity below 30 K is due to trapping of charge carriers in sites characterized by well-defined trapping energies of $E_{b1} = 0.224 \pm 0.003$ eV and $E_{b2} = 0.44 \pm 0.015$ eV. As trapping occurs only below 30 K, the existence of trapping sites does not affect conductivity in cooling; however, they do lead to the observed breaks in resistivity upon warming [17, 18], provided low-temperature charge trapping occurred. The two trapping energies are responsible for the recovery in the vicinity of 70 and 160 K. Some conductivity recovery takes place also above room temperature; however, we could not extract specific trapping energies responsible for the recovery, probably due to the fact that more than one process takes place simultaneously.

We can not identify based on our results what are the trapping sites. A very significant hint, however, is the characteristic length scale. As we noted [11], the low-temperature current- and field-induced conductivity suppression becomes significant in patterns with length scale on the order of microns. Furthermore, in patterns with length scale on the order of 2 microns the conductivity is occasionally suppressed by orders of magnitude. In addition, the conductivity suppression is accompanied by increased spatial variation in conductivity. Therefore, it appears that the trapping sites are related to crystal imperfections of similar length scales. Possible candidates are dislocations that were found to reduce conductivity and mobility of the LAO/STO interface with unusual temperature dependence during warming which is reminiscent to our results [18], or twin boundaries in SrTiO_3 which form due to structural phase transitions of the STO [24–26].

L.K. acknowledges support by the German Israeli Foundation (Grant No. 979/2007) and by the Israel Sci-

ence Foundation founded by the Israel Academy of Sciences and Humanities (Grant No. 577/07). We acknowledge the contribution of Jochen Mannhart and Rainer Jany who provided the samples used for this research.

-
- [1] A. Ohtomo and H. Y. Hwang, *Nature* **427**, 423 (2004).
 - [2] M. Huijben, A. Brinkman, G. Koster, G. Rijnders, H. Hilgenkamp, and D. H. A. Blank, *Adv. Mater.* **21**, 1665 (2009).
 - [3] S. Thiel, G. Hammerl, A. Schmehl, C. W. Schneider, and J. Mannhart, *Science* **313**, 1942 (2006).
 - [4] C. Bell, S. Harashima, Y. Kozuka, M. Kim, B. G. Kim, Y. Hikita, and H.Y. Hwang, *Phys. Rev. Lett.* **103**, 226802 (2009).
 - [5] A. D. Caviglia, S. Gariglio, N. Reyren, D. Jaccard, T. Schneider, M. Gabay, S. Thiel, G. Hammerl, J. Mannhart, and J. -M. Triscone, *Nature* **456**, 624 (2008).
 - [6] T. Schneider, A. D. Caviglia, S. Gariglio, N. Reyren, and J. -M. Triscone, *Phys. Rev. B* **79**, 184502 (2009).
 - [7] M. Ben Shalom, M. Sachs, D. Rakhmilevitch, A. Palevski, and Y. Dagan, *Phys. Rev. Lett.* **104**, 126802 (2010).
 - [8] A. D. Caviglia, M. Gabay, S. Gariglio, N. Reyren, C. Cancellieri, and J. -M. Triscone, *Phys. Rev. Lett.* **104**, 126803 (2010).
 - [9] A. Joshua, S. Pecker, J. Ruhman, E. Altman and S. Ilani, *Nat. Commun.* **3**, 1129 (2012).
 - [10] A. Joshua, J. Ruhman, S. Pecker, E. Altman and S. Ilani, arXiv:1207.7220.
 - [11] S. Seri, M. Schultz, and L. Klein, *Phys. Rev. B* **86**, 085118 (2012).
 - [12] S. Seri and L. Klein, *Phys. Rev. B* **80**, 180410(R) (2009).
 - [13] M. Ben Shalom, E. Levy, A. Palevski, Y. Dagan, C. W. Tai, and Y. Lereah, *Phys. Rev. B* **80**, 140403(R) (2009).
 - [14] X. Wang, W. M. Lü, A. Annadi, Z. Q. Liu, K. Gopinadhan, S. Dhar, T. Venkatesan, and Ariando, *Phys. Rev. B* **84**, 075312 (2011).
 - [15] J. A. Bert, B. Kalisky, C. Bell, M. Kim, Y. Hikita, H. Y. Hwang, and K. A. Moler, *Nature Phys.* **7**, 767 (2011).
 - [16] B. Kalisky, J. A. Bert, B. B. Klopfer, C. Bell, H. K. Sato, M. Hosoda, Y. Hikita, H. Y. Hwang, and K. A. Moler, *Nat. Commun.* **3**, 922 (2012).
 - [17] W. Siemons, G. Koster, H. Yamamoto, T. H. Geballe, D. H. A. Blank, and M. R. Beasley, *Phys. Rev. B* **76**, 155111 (2007).
 - [18] S. Thiel, C. W. Schneider, L. Fitting Kourkoutis, D. A. Muller, N. Reyren, A. D. Caviglia, S. Gariglio, J. -M. Triscone, and J. Mannhart, *Phys. Rev. Lett.* **102**, 046809 (2009).
 - [19] Z. S. Popović, S. Satpathy, and R. M. Martin, *Phys. Rev. Lett.* **101**, 256801 (2008).
 - [20] G. Berner, S. Glawion, J. Walde, F. Pfaff, H. Hollmark, L.-C. Duda, S. Paetel, C. Richter, J. Mannhart, M. Sing, and R. Claessen, *Phys. Rev. B* **82**, 241405(R) (2010).
 - [21] K. Zhou, M. Radovic, J. Schlappa, V. Strocov, R. Frison, J. Mesot, L. Patthey, and T. Schmitt, *Phys. Rev. B* **83**, 201402(R) (2011).
 - [22] J. Biscaras, S. Hurand, C. Feuillet-Palma, A. Rastogi, R. C. Budhani, N. Reyren, E. Lesne, D. LeBoeuf, C. Proust, J. Lesueur, and N. Bergeal, arXiv:1206.1198.

- [23] C. W. Schneider, S. Thiel, G. Hammerl, C. Richter, and J. Mannhart, Appl. Phys. Lett. **89**, 122101 (2006).
- [24] L. Rimai and G. deMars, Phys. Rev. **127**, 702 (1962).
- [25] Farrel W. Lytle, J. Appl. Phys. **35**, 2212 (1964).
- [26] T. Sakudo and H. Unoki, Phys. Rev. Lett. **26**, 851 (1971).